Major Mechanisms of Atmospheric Moisture Transport and Their Role in Extreme Precipitation Events

Luis Gimeno,[1] Francina Dominguez,[2] Raquel Nieto[1,3] Ricardo Trigo,[4] Anita Drumond,[1] Chris J.C. Reason,[5] Andréa S. Taschetto,[6,7] Alexandre M. Ramos,[4] Ramesh Kumar,[8] and José Marengo[9]

[1]Environmental Physics Laboratory, Universidade de Vigo, 32004 Ourense, Spain; email: l.gimeno@uvigo.es, rnieto@uvigo.es, anitadru@uvigo.es

[2]Department of Atmospheric Sciences, University of Illinois, Urbana, Illinois 61801-3070; email: francina@illinois.edu

[3]Department of Atmospheric Sciences, Institute of Astronomy, Geophysics and Atmospheric Sciences, University of São Paulo, 05508-090 São Paulo, Brazil

[4]Instituto Dom Luiz, Universidade de Lisboa, 1749-016 Lisboa, Portugal; email: rmtrigo@fc.ul.pt, amramos@fc.ul.pt

[5]Department of Oceanography, University of Cape Town, 7701 RSA, South Africa; email: chris.reason@uct.ac.za

[6]Climate Change Research Centre, University of New South Wales, 2052 Sydney, Australia; email: a.taschetto@unsw.edu.au

[7]Australian Research Council Centre of Excellence for Climate System Science, University of New South Wales, 2052 Sydney, Australia

[8]National Institute of Oceanography, Dona Paula, 403004 Goa, India; email: kramesh@nio.org

[9]National Center for Monitoring and Early Warning of Natural Disasters, 12630-000 São Paulo, Brazil; email: jose.marengo@cemaden.gov.br

Annu. Rev. Environ. Resour. 2016. 41:117–41

First published online as a Review in Advance on July 6, 2016

The *Annual Review of Environment and Resources* is online at environ.annualreviews.org

This article's doi: 10.1146/annurev-environ-110615-085558

Keywords

atmospheric moisture transport, atmospheric rivers, low-level jets, precipitation extremes, floods, droughts

Abstract

We review the major conceptual models of atmospheric moisture transport, which describe the link between evaporation from the ocean and precipitation over the continents. We begin by summarizing some of the basic aspects of the structure and geographical distribution of the two major mechanisms of atmospheric moisture transport, namely low-level jets (LLJs) and atmospheric rivers (ARs). We then focus on a regional analysis of the role of these mechanisms in extreme precipitation events with particular

attention to the intensification (or reduction) of moisture transport and the outcome, in terms of precipitation anomalies and subsequent flooding (drought), and consider changes in the position and occurrence of LLJs and ARs with respect to any associated flooding or drought. We then conclude with a graphical summary of the impacts of precipitation extremes, highlighting the usefulness of this information to hydrologists and policymakers, and describe some future research challenges including the effects of possible changes to ARs and LLJs within the context of future warmer climates.

Contents

1. INTRODUCTION

Each of the main components of the hydrological cycle plays a major role in the global climate system (1). Thus, considered from the perspective of climate change and variability, it is of the utmost importance to obtain the best possible understanding of both the intensity of the hydrological cycle and its evolution over time. Indeed, this could be said to represent one of the most important challenges for research in geoscience for this century. Understanding the processes governing the evaporation of water from the oceans (2) and the transport of atmospheric moisture (3) is particularly important, as is understanding the effects of each of these processes on the hydrological cycle (4)—all within the context of the current paradigm of global climate change (5).

The transport of moisture from the oceans to the continents is the primary component of the atmospheric branch of the water cycle and forms the link between evaporation from the ocean and precipitation over the continents (1). A detailed study of this transport could provide both a better understanding of any observed changes and some physical evidence in support of the many available projections of future climates (e.g., 6–8). Understanding the physical processes behind transport of moisture can lead to improved rainfall forecast in monsoon regions for a firmer grasp of the monsoonal precipitation that plays a significant role in both local continental evaporation and the transport of vapor from adjacent oceanic regions (e.g., 9). A better understanding of the role of anomalies in the transport of moisture as observed during natural hydrometeorological hazards is also required, in relation to extreme drought (e.g., 10) or intense precipitation (11).

A review of the conceptual models of moisture transport is required to underpin any study of the origins of continental precipitation. Of the two large-scale dynamical/meteorological structures known to play important roles, namely low-level jet (LLJ) systems and atmospheric rivers (ARs), the former are known to be key in tropical and subtropical regions. The characteristics of LLJs and their associated transport of moisture have been described in several regions (e.g., 12, 13). ARs are also important in the transport of moisture, although these structures are mostly confined to extratropical regions (14). A large proportion of extreme precipitation events in the Western United States (e.g., 15) and Western Europe (16) are now thought to be linked to the occurrence of ARs, including some famous historical floods (e.g., 17). Overall, the contributions of ARs and LLJs to total precipitation at the regional scale are not yet well quantified and are likely to be larger than previously considered. Moreover, there has never been any attempt to unify our understanding of these processes at the global level, and a global assessment is therefore one of our aims here.

The transport of moisture by ARs and LLJs is also connected to monsoonal regimes and to other important natural hazards. It has been suggested that there are two main sources of monsoonal precipitation, namely local continental evaporation and transport from adjacent oceanic regions (e.g., 9, 18). Several researchers have identified low levels of moisture transport during the active phases of monsoon regimes (e.g., 19). There is nevertheless a degree of uncertainty concerning the mechanisms involved in the anomalies of moisture transport seen during precipitation extremes and their consequences (i.e., drought or flooding). Drought occurs when there is significantly less moisture available than normal for long periods and the demand for water cannot be met (20), whereas the transport of large amounts of water vapor and its associated convergence may trigger extreme rainfall events and cause flooding (21). The persistence of drought could be due in part to a lack of transport to the continents (22) as seen during the most recent major drought in the Iberian Peninsula (10) and southeastern Brazil (23).

In this review we focus on the two major mechanisms of atmospheric moisture transport, i.e., LLJs and ARs, and discuss their roles in extreme hydrometeorological events (droughts and flooding) at the global scale. We pay particular attention to (*a*) the intensification (or reduction) of moisture transport caused by each, together with their role in rainfall anomalies and flooding (drought); (*b*) changes in the position and occurrence of LLJs and ARs and associated rainfall response and flooding and drought; and (*c*) possible changes affecting ARs and LLJs within the context of future warmer climates.

2. GENERAL OVERVIEW OF MAJOR ATMOSPHERIC MOISTURE TRANSPORT MECHANISMS

2.1. Atmospheric Rivers

ARs are relatively narrow atmospheric corridors along which much of the atmospheric water vapor is transported from the subtropics to the midlatitudes (24). It is generally accepted that more than 90% of the total midlatitude vertically integrated water vapor (IWV) flux is transported by these structures. A wide range of alternative terms have been used for this meteorological phenomenon over the past few decades, including tropospheric rivers (25), tropical moisture exports (TMEs) (26), and moisture conveyor belts (27). At a more regional scale, ARs have also been given local names such as Hawaiian Fire Hose, Pineapple Express (28), and Maya Express (29). Nevertheless, the term atmospheric river is now widely accepted, implying the ability of these structures to transport water in the atmosphere at rates similar to those seen in the largest rivers of the world (24, 30). ARs supply water vapor, bringing large amounts of precipitation and often contributing to extreme precipitation events, causing flooding, inducing landslides, and damaging ecosystems.

However, ARs also play a critical role in water supply for regions such as California and Arizona in the United States and Baja California in Mexico (15, 31, 32).

Over the past few decades, there have been several publications regarding the structure of ARs, and Gimeno et al. (14) provide a complete list of observational and modeling results. In essence, ARs are shallow (1–2.5 km in height) and narrow (∼300–500 km in width) plumes with high water vapor contents, stretching over distances of at least 2,000 km, and are often associated with the pre-cold-frontal region of extratropical cyclones in the region of the warm conveyor belt (WCB) (33). ARs are always associated with strong winds at low levels of the atmosphere, whereas an LLJ is positioned ahead of the maximum moisture flux (**Figure 1**) due to the temperature gradient across the cold front. This produces a concentrated band of intense low-level-specific humidity and a vertical distribution of equivalent potential temperature (34, 35) showing subsidence at low levels ahead of the AR, a low-level potential instability on the rear part of the front, and a moist-neutral stratification in the area of the AR. In the context of ARs, it is important to highlight the relationship between WCBs and TMEs, as recently proposed by a small group of experts at the International Atmospheric Rivers Workshop, where a consensus was reached on the definition of each component (36 , pp. 1–2):

> The WCB refers to the zone of dynamically uplifted heat and vapor transport close to a midlatitude cyclone. The vapor is often transported to the WCB by an AR, and the result of the uplift is heavy rainout that generally marks the downwind end of AR conditions if the AR hasn't experienced orographic uplift (upslope flow) and rainout over mountains earlier along its approach to the WCB. TMEs are zones of intense vapor transport out of the tropics, vapor that is frequently conducted by ARs toward cyclones and WCBs. TMEs can provide important vapor sources for ARs, but most ARs also incorporate midlatitude sources and convergences of vapor along their path.

Two main approaches are generally used to detect ARs using an objective analysis. The first is based on the computation of the IWV (e.g., 15, 35, 37); the second uses the vertically integrated horizontal water vapor transport between two atmospheric levels (e.g., 16, 24, 38, 39). A recent review presented an exhaustive summary of the main methodologies used (14).

Typically, between three and five ARs occur in each hemisphere simultaneously. Intense ARs with particular meteorological relevance in terms of precipitation are more frequent in winter. Even though the IWV in the ARs is sometimes greater in summer, the vapor flux is stronger in winter due to the stronger flows associated with extratropical cyclones. During the cold season, ARs are associated with a winter planetary wave number of 4–5 (24). Regions affected by extratropical cyclones are therefore potential areas of AR occurrence. In the past two decades, maps showing the general distribution of ARs have been produced (e.g., 24, 40), and these were also summarized in the recent works of Gimeno et al. (14) and of Guan & Waliser (39). **Figure 2** illustrates the main regions of their occurrence. ARs are generally detected along the eastern borders of the Atlantic and Pacific oceans, in the western north and south Atlantic, on both sides of the Indian Ocean (in South Africa and Australia), and on the coast of Japan. There are additional structures of moisture transport over regions such as the Indian Peninsula and the Caribbean, but these are related more to monsoonal regimes and LLJs; therefore, strictly speaking, they are not ARs.

Through orographic lifting, ARs can produce large amounts of precipitation when they reach coastal areas. However, this is not the only mechanism inducing the upward motion of moisture; other processes such as synoptic and mesoscale systems can play an important role in the intensification of precipitation via the associated convective motion, and mesoscale frontal waves can modify the stability or the duration of ARs (41). The past few years have seen an increasing number of studies showing the continental areas particularly affected by ARs (e.g., 14, 39). Three areas have emerged from this work in particular, namely the west coast of North America

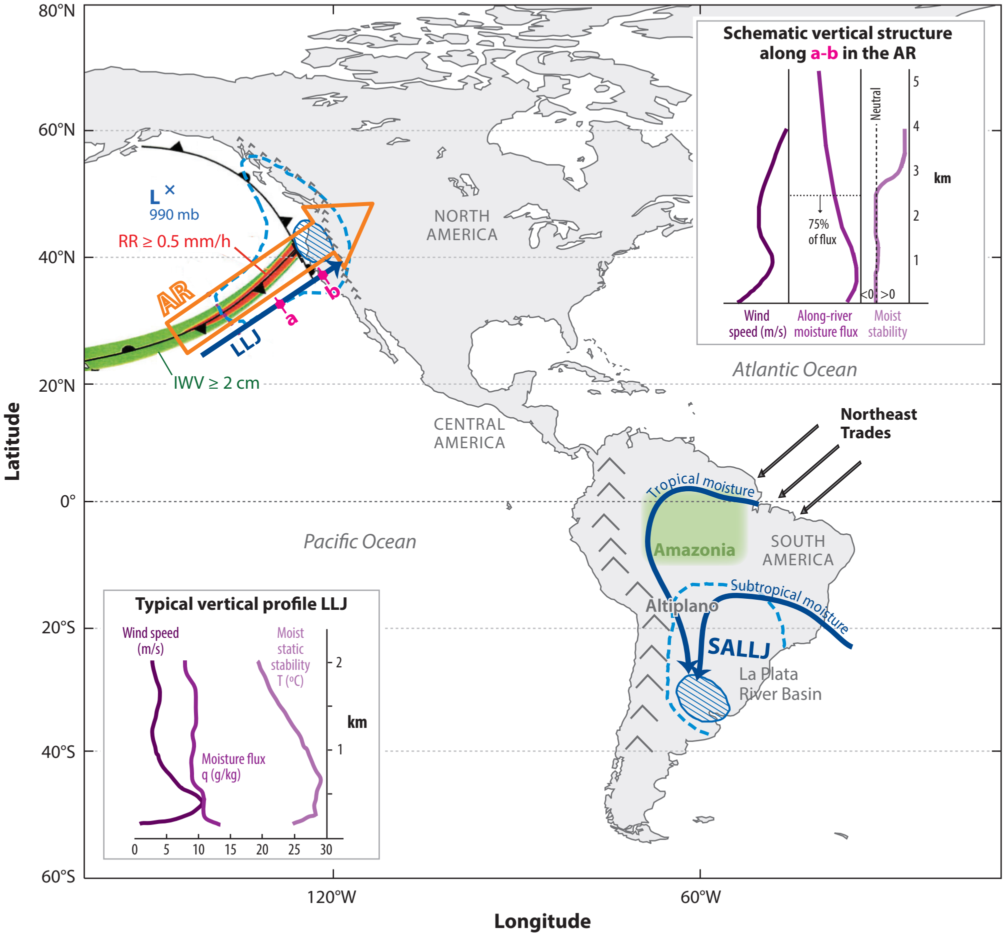

Figure 1

Conceptual model of an atmospheric river (AR) over the Northern Pacific coast in North America and of a low-level jet (LLJ) over South America. AR: Schematic view of the positions of the polar cold front (*black*) and the associated LLJ (*dark blue*). The orange arrow shows the AR. The cross and L in blue indicate the relative position of a low-level pressure of 990 mb. The integrated total column of water vapor (IWV) ≥2 cm is shown in green and the associated rain-rate enhancement (RR) ≥0.5 mm/h along the AR is shown in red. The precipitation area associated with the AR is denoted by the dashed blue line (*diagonal stripes* indicate intense precipitation). The pink line a–b marks the limits where the profiles for the top inset are integrated: (*dark purple*) the wind speed, (*purple*) the vertical structure of the moisture flux, and (*light purple*) the moist stability. South American low-level jet (SALLJ): Schematic view of the moisture transport into South America from the tropical and subtropical South Atlantic Ocean that form the LLJ along the Andes. Thin black arrows represent the Northeast Trades. The precipitation area associated with the LLJ is denoted by the dashed blue lines (*diagonal stripes* indicate intense precipitation). (*bottom*, *inset*) A typical vertical profile of an LLJ is shown including wind speed (*dark purple*; in m/s), moisture flux (*purple*; in g/kg), and moist static stability temperature (*light purple*; in °C). The ARs are adapted from Reference 35, figure 23*a*, and Reference 34, figure 13*b*. The SALLJ is adapted from Reference 18, figure 1, and Reference 160, figure 1*b*.

(39, 42, 43), Western Europe (16, 39), and southwestern South America (39). Moreover, and as seen in **Figure 2**, several other locations are affected by ARs as previously detected and analyzed, and these are further addressed in Section 3, together with their impacts. **Figure 2** shows that ARs also have a high impact in regions such as the Gulf of Mexico, Greenland, Antarctica, and other areas that have received relatively little attention in the previous literature, such as Australia

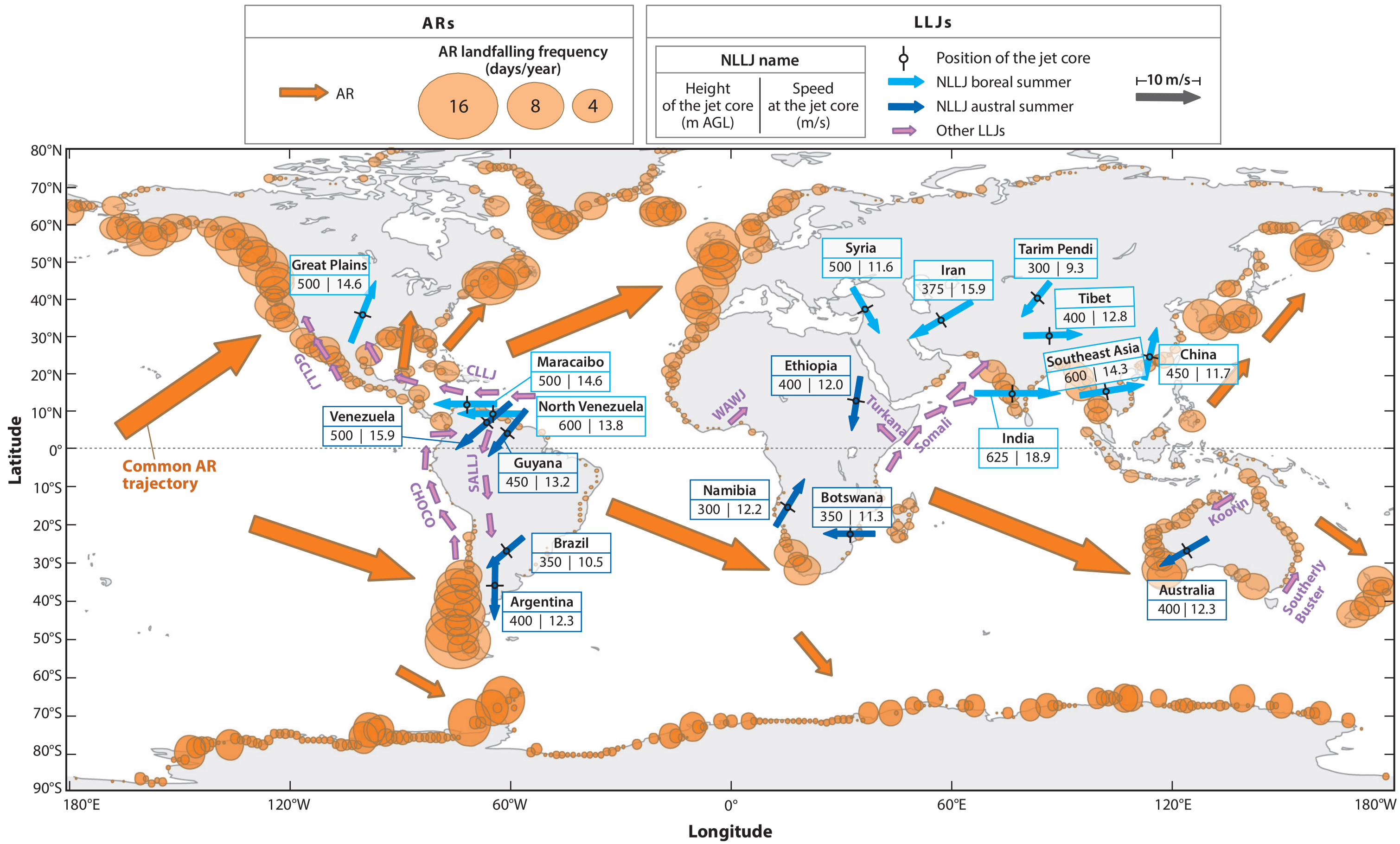

Figure 2

The global geographical position of atmospheric rivers (ARs) and low-level jets (LLJs). ARs are shown by the large orange arrows. Each arrow denotes the direction of flow. The figure is based on References 24 and 38 and several maps of integrated total column of water vapor (IWV) composites. Orange circles denote the frequency (days/year) of AR landfalling (39). LLJs: Blue arrows show the locations of night low-level jets (NLLJs), as described for summer in Reference 54 (*light blue*, Northern Hemisphere; *dark blue*, Southern Hemisphere). The name of the jet (colored boxes next to arrows), its typical height [*bottom-left*; in m AGL (above ground level)], and its typical speed (*bottom-right*; in m/s) at the jet core are also displayed. The size of the arrow is scaled with respect to speed. These characteristics together with the position of the jet core were obtained from Reference 54, table 2. (*purple*) Other LLJs with high climatic relevance: the Great Plains low-level jet (GPLLJ), Gulf of California low-level jet (GCLLJ), Caribbean low-level jet (CLLJ), CHOCO low-level jet (CHOCO LLJ), South American low-level jet (SALLJ), Turkana low-level jet (Turkana LLJ), Somali low-level jet (Somali LLJ), Koorin low-level jet, and Southerly Buster.

and New Zealand, southwestern South Africa, the Pacific coast of Asia, and northeastern North America (39).

Several authors have shown how a few major modes of climate variability may significantly influence the occurrence of ARs. The Arctic Oscillation and the Pacific/North American teleconnection pattern in their negative phases increase the number of winter ARs in the western United States in comparison with the positive phases of these modes (90% and 50%, respectively) (39). A regional study of the British Isles showed that the impact of the Scandinavian (SCAN) negative phase contributes to increasing ARs in this area (40). The North Atlantic Oscillation (NAO) impinges its "seesaw" behavior on the occurrence of ARs in Europe (44), with an increase in ARs affecting southern Europe during its negative phase and an increase in northern Europe when the NAO is in its positive phase. For the particular case of the Iberian Peninsula, the East Atlantic teleconnection pattern plays a more determinant role than the NAO with respect to the interannual variability of the frequency of ARs (38). During an El Niño event [the warm phase of the El Niño–Southern Oscillation (ENSO)], the frequency of ARs increases over subtropical and extratropical regions, with the opposite behavior during La Niña (the cold phase). During an El Niño event, more anomalies in terms of the number of ARs are seen over the northeastern Pacific, the north Atlantic, and the Gulf of Mexico. The impact of land falling systems is stronger in terms of precipitation in the northwest United States and western Canada but decreases over California (27, 32, 39). During the neutral phase of the ENSO, the transport of moisture from the tropics to the pole is favored, and ARs appear to be more common (42, 27, 32). Future changes in the occurrence of ARs in the context of climate change, including heavy and prolonged precipitation episodes associated with ARs, have also been modeled under future climate scenarios (e.g., 45, 46) to analyze future changes in ARs and to highlight any possible implications.

2.2. Low-Level Jets

The wind corridors of the lower atmosphere are generally termed LLJs, and these carry much of the moisture transport from low to high latitudes or from warm oceans toward continental areas (**Figure 2**). Different definitions of LLJs are found in the literature (47). LLJ was first defined as a "significant" wind maximum within the first 1.5 km of the atmosphere, decreasing by at least five knots to the next minimum at a higher level (48). Bonner's (49) extensively adopted criterion is quite similar and includes the magnitude and vertical shear of the wind, which must exceed 12 m/s and decrease by at least 6 m/s to the next higher-level minimum or to the 3-km level—whichever is lower. Whiteman et al. (50) adopted Bonner's definition but added a weaker category of LLJs.

LLJs are primarily a warm-season phenomenon, and the mechanisms that drive them differ between coastal and inland jets (47). Coastal LLJs are generally in geostrophic balance and are associated with topography and with daily cycles of land–sea contrast (e.g., 51). On the other hand, jets located inland within continents are generally driven by topographic and/or inertial effects or may result from secondary circulations associated with upper-level flows (52). Topography may influence the behavior of an inland jet in different ways. For example, several LLJs are the result of channeling through gaps in the terrain via the Bernoulli effect (e.g., over central Iran; see 53). Barrier jets flow parallel to the topography and often result from geostrophic adjustment (e.g., the South American LLJ east of the Andes; see 13, 18).

The most commonly studied LLJs are those that achieve their maximum strength at night, forming at least in part from the decoupling of the planetary boundary layer after sunset; we refer to these as nocturnal low-level jets (NLLJs) (54). NLLJs tend to have maxima near local midnight, with the height of the jet core ranging from 300 to 600 m above ground level (AGL), with a mesoscale and synoptic-scale extent. Two major mechanisms favor the generation of NLLJs; the first depends on the decoupling and eventual recoupling of the lower troposphere to the surface through diurnally varying eddy viscosity driven by changes in solar heating (48), and the second is related to the response to changes in horizontal baroclinicity arising from spatial contrasts in insolation and horizontal variations in the topography.

The lack of data at high temporal and spatial resolutions means that the proper study of NLLJs remains a particular challenge. There are a few exceptions for some systems where high-resolution observational data are available, such as for the LLJ for the Great Plains of North America (e.g., 55, 56), or where concerted field campaigns have been used, such as for the South American LLJ east of the Andes (e.g., 57). However, to overcome the problem of data scarcity, Rife et al. (54) made use of 21 years of global downscaled reanalysis data with a horizontal resolution of 40 km at hourly intervals to document the characteristics of NLLJs over the entire planet. An index of NLLJ activity was proposed based on the vertical structure of the temporal variation of the wind. On the basis of the methodology proposed by Whiteman et al. (50), two criteria must be satisfied simultaneously: The first requires the winds at 500 m AGL (near jet level) to be stronger at local midnight than at local noon, and the second requires the wind speed at the core of the jet (500 m AGL) to be stronger than that at a higher level (4 km AGL). This technique was used to resolve not only all the NLLJs known previously (12), but also some newly identified jets, including those over Ethiopia, Colombia, Venezuela, Guyana, Syria, Iran, Tarim Pendi, Tibet, the Brazilian Highlands, and the Great Rift Valley in Africa. **Figure 2** shows the mean characteristics (strength and direction, and the position and velocity of the core jet) for each of these 18 NLLJs considered. Most of the NLLJs occur in the Northern Hemisphere because of the stronger land–sea temperature contrasts generated by the larger continental expanses. Also, NLLJs predominantly occur within 30° of the equator. Equatorward of 30°, diurnal land–sea variations produce inertia-gravity waves that can propagate far from their origin (58). Poleward of 30°, the atmospheric response is more localized (e.g., a land–sea breeze).

Numerous authors have documented the linkage between NLLJs and rainfall in different regions, such as in the Great Plains (e.g., 56, 59), South America (e.g., 60), Africa (61), India (62), and the western Pacific (63). Monaghan et al. (64) introduced a statistical approach to categorize nocturnal precipitation extremes as a function of NLLJ magnitude, wind direction, and wind frequency. They found that relationships between NLLJs and nocturnal precipitation extremes exist in at least ten regions around the world, including the US Great Plains, Tibet, northwest China, India, Southeast Asia, Southeast China, Argentina, Namibia, Botswana, and Ethiopia. According to this study, "For many jets, we have shown a physical linkage exists between the jet exit region and enhanced precipitation. Previous studies have shown that mesoscale ascending motion often occurs near the terminus of the NLLJ either because of the jet encountering an upward terrain slope or a frontal zone. However, for other jets, such as those found in Guyana, Venezuela, Australia, India, and Brazil, the relationship to the jet exit region is unclear. Interestingly, all these regions have a significant coastal influence. In many coastal regions, the diurnal cycle within the coastal zone tends to produce convection onshore during the daytime and offshore at night" (64, p. 5083).

3. REGIONAL STUDIES

3.1. North America

The seasonality of the precipitation over the continental United States is strongly modulated by the transport of moisture from the subtropical and tropical oceans to the continental land mass. Early observational studies showed that a significant moisture flux into the United States during the summer season arrives as a southerly flow from the Gulf of Mexico (65). Station observations provided further evidence that from April to September, the South Central United States experiences nocturnal southerly wind maxima (sometimes in excess of 20 m/s) between 200 and 1,000 m above the surface, known as the Great Plains low-level jet (GPLLJ). The GPLLJ (**Figure 2**) arises due to the strong pressure gradient at the western edge of the North Atlantic subtropical high and interactions with the complex terrain of the Rocky Mountains and the diurnal variations of eddy viscosity within the boundary layer (66).

The GPLLJ plays a critical role in the hydrological cycle of the central United States. In a two-month (May–June) global circulation model simulation, the GPLLJ was shown to bring in roughly one-third of all the moisture entering the continental United States (66). The jet has been extensively linked to precipitation throughout the region (56). Summer rainfall shows an early evening peak over the Rocky Mountains and a near-midnight peak in the Central Plains of the United States, with more than 25% additional precipitation at night than during the day—associated with the GPLLJ (56). In fact, parts of the Midwest and the Central Plains receive more than 30% of their total nighttime rainfall during the strongest LLJs, which are relatively infrequent (56). LLJs are most frequent in a large region extending from the Mexico-US border to the upper Midwest, on the eastern slopes of the Rocky Mountains (49). However, the continental part of the enhanced LLJ-associated rainfall is variable and migrates from the north central states in May to the southern and eastern states in July and August. This migration follows enhanced moisture flux and synoptic-scale patterns (56).

There is a well-known inverse relationship between the GPLLJ and the Gulf of California low-level jet (GCLLJ; **Figure 2**), the latter influencing precipitation in the southwestern United States and in northwestern Mexico (55). When the GCLLJ is strong and precipitation increases over Arizona, the GPLLJ is weak and precipitation decreases over the Great Plains; however, the relationship is not symmetrical, and a strong GPLLJ is not related to a weaker GCLLJ (55). GCLLJ events are characterized by strong southerly winds that extend along the entire Gulf of California throughout the bottom 1–2 km of the atmosphere and extend into Arizona, southeast California and southern Nevada (67). The high winds of the GCLLJ can cause dust transport and reduced visibility, but when associated with moisture transport the jet is regionally known as a gulf surge event and brings a much-needed drop in temperature and an increase in moisture to the Sonoran Desert (68–70). Active and break periods are typical during the monsoon season (71, 72). Gulf surges are one of the principal mechanisms responsible for the strong advection of moisture and active periods of precipitation during the North American monsoon season (70). Furthermore, recent research has found that a large proportion of gulf surge events are related to tropical cyclones, suggesting a mechanism by which tropical cyclone moisture can be channeled into the southwestern United States (69, 73–76).

Periods of extreme precipitation over the central United States (**Figure 3**) are linked to intensified GPLLJ moisture transport and moisture convergence downwind of the GPLLJ (77). Indeed, the GPLLJ played a critical role in the 1993 floods that affected the American Midwest when the region experienced an increased incidence of very strong LLJs in late June and early July (77, 78). However, extreme flooding in the Midwest is not just a regional phenomenon; it is also a part of large-scale patterns that link tropics and the midlatitudes via long-range moisture transport from areas as remote as the Caribbean Sea (79). Moisture sources for the extreme flooding events of 1993 and 2008 were associated with this significant pathway known as the Maya Express that extends from the Caribbean Sea to Central America and then joins the GPLLJ as it enters the United States (79, 80). Understanding these events as part of a large-scale pattern of moisture transport is in line with the idea that the GPLLJ is the northerly branch of the Caribbean low-level jet (CLLJ) as it crosses the Yucatan Peninsula and veers north into the United States (81).The Maya Express

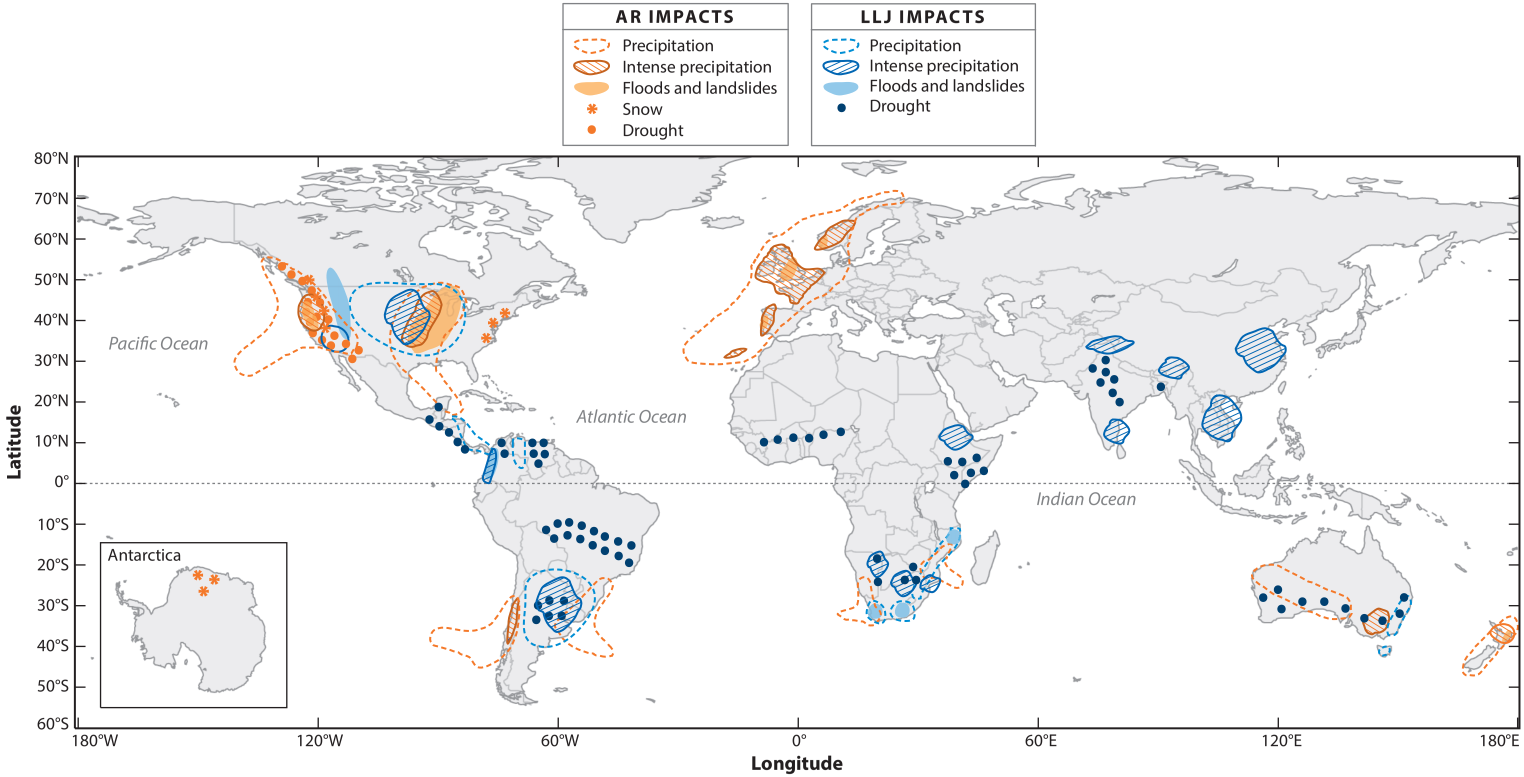

Figure 3

Summary of the general impacts of extremes linked to atmospheric rivers (ARs) (*orange*) and low-level jets (LLJs) (*blue*) in terms of precipitation (*dashed outline*), intense precipitation (*diagonal stripes*), floods and landslides (*solid color*), snow (*asterisks*), and drought (*dots*).

is essentially the local name for the AR structures (**Figure 1**) that have recently been linked to the most extreme spring and summer flooding events throughout the region (82).

During the past decades, the GPLLJ has strengthened and suffered a northward migration in spring (April–June). This pattern implies that over the Southern Plains droughts are more common, whereas precipitation increases in the Northern Plains (83).

Unlike the GPLLJ or the GCLLJ, ARs are not confined to a specific region and have no clear diurnal cycle. Perhaps the best known is the Pineapple Express (43), which can be often clearly identified from satellite imagery as a long filament of water vapor connecting the Hawaiian Islands with western North America.

ARs have been extensively associated with extreme winter precipitation and flooding events (**Figure 3**) throughout the western coast of the United States, undoubtedly the region that has been the focus of the most attention (15, 84, 85)—in stark contrast to ARs in the central United States, which are spring and summer phenomena. In an analysis of four major watersheds in the western state of Washington, almost all the annual peak daily flow events were associated with ARs, and these events were characterized by above-normal temperatures that led to significant rain—as opposed to snow—causing flooding in the region (86). The role of the orientation of an AR in relation to topography has been shown to be a critical factor affecting the probability of flooding (86, 87).

More recently, ARs have been linked to extreme floods in more inland locations of the southwestern United States (31, 87, 88, 89). However, ARs in the southwestern United States can differ greatly from those affecting the West Coast because moisture can be transported at mid-levels in association with cutoff lows off the coast of California and Baja California (31, 32, 90). Although ARs are linked to extreme rainfall and flooding, they also play a critical role in water resources in the southwestern United States—this region is critically dependent on winter precipitation, and just a few of these extreme storms can bring most of the annual rainfall (15). These studies of ARs have led to numerous significant conclusions about their impacts (**Figure 3**), including the recognition that (*a*) ARs cause the majority of the flooding seen in rivers all along the American West Coast (42 , 91), (*b*) ARs represent the source of 30–50% of all the precipitation in this region (15), and (*c*) ARs are frequently the cause of the end of drought periods on the West Coast (92).

3.2. Central and South America

Several jets modulate the climatology of Central and South America. The LLJs identified over this region are the CLLJ (see 93 for a review), the CHOCO LLJ (see 94 for a review), and the South American low-level jet (SALLJ) (see 13 for a review). South America is also affected by ARs mainly at subtropical latitudes (95).

The precipitation over the Pacific coast of Colombia is determined by the low-level westerly (CHOCO) jet. The transequatorial winds blowing over the Pacific Ocean acquire a west–east trajectory and penetrate Colombia as an LLJ (94). The CHOCO LLJ has a long pathway; it has been detected as far south as 30°S near the Chilean coast (96).The jet has a wind maximum at 900–1,000 hPa and is associated with strong land–ocean temperature gradients and therefore with a baroclinicity surface. This jet presents a very strong annual cycle, being imperceptible in February–April and intensifying from May to a peak in October–November (94). The long-term average transport of moisture has been estimated to be approximately 3,800 m^3/s, which helps explain the existence of one of the rainiest areas of the planet along the Pacific coast of Colombia and the development of strong erosion on the Western Cordillera of the Colombian Andes. The CHOCO LLJ is also able to transport moisture into southern Central America during boreal summer and autumn (97). Due to its position, the flow is highly modified by the ENSO phenomenon.

Over the Caribbean Sea, the CLLJ is located between northern South America and the Greater Antilles. This jet is responsible for the moisture transport from the tropical Atlantic Ocean into the Caribbean Sea and the Gulf of Mexico (east–west direction); its axis is located at 15°N, and the intensified winds are confined below 600 mb, with maximum values below 925 mb. The flow reaches the eastern Pacific, crossing Central America (95). It exhibits a very marked seasonal pattern after splitting into two main branches when it reaches the western Gulf of Mexico; during boreal summer the first of these branches turns to the north reaching the central United States and becoming the GPLLJ. During boreal winter, the northeast trades blow across the Isthmus of Tehuantepec, and three distinct wind jets result from the major gaps in the Central American mountain range, one of which then merges with the CHOCO jet. The CLLJ is the regional climate modulator during summer when the jet is intensified and is responsible for the maximum precipitation over the Caribbean coast of Nicaragua and Costa Rica when convergence occurs in the jet, with reduced precipitation in the case of low-level divergence (93).

The easterly trade winds from the tropical Atlantic Ocean penetrate into northern South America and flow along the eastern border of the Andes, crossing Amazonia and reaching the La Plata River Basin (see **Figure 1**). This flow develops the structure of an LLJ and is called the South American LLJ east of the Andes (SALLJ) (13, 57).

Moisture transport into and out of the Amazon basin has been studied since the 1990s using a variety of upper air and global reanalysis datasets, as well as data from climate model simulations. During the wet season in particular, moisture is exported from the Amazon basin and transported via the SALLJ east of the Andes, contributing to precipitation over southern Amazonia and the La Plata River Basin (13, 30, 80, 98–102). During the major drought in southern Amazonia in the summer of 2005, the number of SALLJ events during January 2005, at the height of the peak of the rainy season, was zero, suggesting a disruption of the moisture transport from the tropical North Atlantic into southern Amazonia during that summer (103).

Changes in land use—particularly deforestation in the Amazon basin—alter the rate of evapotranspiration and affect the water cycle (104, 105). Some authors have suggested that the dominant sources of monsoonal precipitation are local continental evaporation and the transport of vapor from adjacent oceanic regions (e.g., 18). The resulting reduction in regional moisture from the tropical North Atlantic supply may have important consequences for the stability of the Amazonian rainforests and also for other southern regions depending on the Amazon rainforest as a moisture source. Thus, when the wide Amazon basin receives significantly less precipitation and becomes drier than usual, it can potentially induce extreme droughts in those regions that depend on the Amazonian moisture, as is the case of the La Plata River Basin (106). Any anomaly in the moisture transport by the SALLJ may lead to extreme droughts due to lack of precipitation or may promote, simultaneously, excessive precipitation in other regions (107).

ARs are also important for the transport of moisture in extratropical regions (14, 39). The heavy winter orographic precipitation events over Central Chile (Andes area) are strongly related to an intense water vapor transport from the southern Pacific in the form of an AR associated with extratropical cyclones (108). The most intense rainfall tends to occur near and above the crest of a mountain range (109).

3.3. Europe

The intra- and interannual variability of European precipitation are both strongly affected by the transport of moisture from the North Atlantic and the Mediterranean into Europe (8). However, whereas the North Atlantic moisture source affects the entire continent of Europe mostly in winter, the Mediterranean source affects southern Europe in both winter and summer. One of the major mechanisms associated with moisture transport from the North Atlantic toward Europe are ARs (**Figure 2**), usually embedded in the trailing fronts of extratropical cyclones. Despite the importance of ARs in atmospheric moisture transport, the analysis of their contribution to precipitation in Europe has generally been restricted to a few specific extreme events (e.g., 21, 110). Only in the past few years have any long-term climatological studies been published (e.g., 38, 44).

ARs are responsible for approximately 20–30% of all the precipitation in parts of Western Europe, with the maximum being recorded in autumn and winter (mainly in France and the Iberian Peninsula) and the effects of ARs generally being felt further inland (e.g., Poland) than in the western United States. This is most likely a result of the blocking role played by the higher mountainous terrain in the latter, which acts as a barrier to inland penetration (111). In addition, there is a strong relationship between ARs and the occurrence of annual maximum precipitation days in Western Europe, which is particularly pronounced along the coast, where some areas had eight of their ten highest annual maximum precipitation days related to ARs (44).

In terms of local climatological studies, three areas have received particular attention: (*a*) the British Isles (16, 40); (*b*) the Iberian Peninsula, where daily precipitation extreme events were associated with ARs in different domains (38, 112); and (*c*) Madeira Island, where precipitation over a 10-year period was associated with meridional water vapor transport in ARs during the winter (113). ARs have also been detected using different reanalysis datasets such as Era-Interim, NCEP/NCAR reanalysis (38, 40), and even the Twentieth-Century Reanalysis Project (17).

Lagrangian analysis has also been applied to ARs in Europe at different timescales. Sources of water vapor producing precipitation over Norway and the link with ARs were investigated over a five-year period (21). A similar approach was used to analyze moisture origin and meridional transport in ARs and their association with multiple cyclones in December 2006 (114). A Lagrangian climatology of TMEs (in AR-like structures) to the Northern Hemispheric extratropics was developed (26) by analyzing forward trajectories leaving the region between 0° and 20°N for the period 1979–2001. A backward trajectory approach was applied to study where the ARs uptake anomalously moisture that reached different parts of Western Europe (115).

The importance of ARs in different extreme precipitation events in Europe was also analyzed in detail to evaluate the extreme precipitation event that took place in the city of Lisbon (Portugal) in November 1983 (110), which produced flash flooding, urban inundations, and landslides, all of which caused considerable damage to infrastructure and led to some fatalities. This work showed that this unusual event was clearly associated with the transport of tropical and subtropical moisture by an AR associated with an extratropical cyclone. Two historical floods in the Iberian Peninsula are clearly associated with ARs. The first in December 1876 affected the southwestern sector of the Iberian Peninsula, leading to the highest discharge ever recorded in two large international rivers (Tagus and Guadiana), with a significant socioeconomic impact (17). The second affected the northwestern sector of the Iberian Peninsula on December 20–28, 1909, and was the hydrogeomorphological event with the highest number of flood and landslides recorded in Portugal over the period 1865–2010 (116). This event also caused important social impacts in parts of Spain, especially in the Douro basin, having triggered the highest floods in more than 100 years at the river mouth in the city of Oporto (117). The intense precipitation and flash flood event of February 20, 2010, in Madeira caused more than 40 deaths, with many missing and injured, as well as a vast range of material losses, including the destruction of houses, industries, roads, bridges, and several thousand vehicles (118).

LLJs are not significant in terms of atmospheric moisture transport in Europe. Some LLJs can be identified, mainly offshore, such as in the Iberian Peninsula (119) or in Norway (120). These have some relevance for offshore wind installations and energy production.

3.4. Africa

The climate of tropical Africa is dominated by the movement of the Intertropical Convergence Zone (ITCZ) and the monsoonal regimes that affect West and much of East Africa. To the north of this monsoon-influenced region lies the Sahara Desert. To its south, southern Africa is essentially a narrow, peninsula-like landmass surrounded on three sides by oceans. Its climate, its marine and terrestrial ecosystems, and its economy are all strongly influenced by this land–sea configuration and associated marine influences. Although the Indian Ocean has traditionally received the most scientific attention as the major oceanic moisture source for southern African summer rainfall (121), the South Atlantic and the Southern Ocean also play important roles (122). Most of the landmass receives the bulk of its rainfall during the austral summer, but the western part of South Africa mainly receives winter rainfall, and the south coast experiences rainfall throughout the year. However, a bimodal rainfall regime occurs near the equator in Tanzania and the Eastern Congo Basin.

The seasonality of this precipitation is largely controlled by movements in the ITCZ and the subtropical semipermanent anticyclones over the South Atlantic and South Indian oceans. At seasonal scales, the major oceanic moisture sources for summer rainfall are the tropical Western Indian Ocean (123), the subtropical Southwest Indian Ocean, and to a lesser extent the tropical Southeast Atlantic Ocean (124). Inflow from the latter is facilitated by the development of a thermal low over northern Namibia/southern Angola in the Angola low in austral spring, which typically persists until late autumn. A secondary convergence zone links this feature with the meridional arm of the ITCZ that passes through the Eastern Congo Basin.

As is common elsewhere in the tropics and subtropics, the rainy season is made up of numerous wet and dry spells. Wet spells over South Africa during summer tend to be associated with an inflow of moisture (see **Figure 2**) from the tropical Southeast Atlantic (Namibia jet) that converges over the land mass with the mean easterly moisture inflow from the Indian Ocean (Botswana jet) (124). During southern African drought periods, moisture fluxes from the western Indian Ocean are much reduced. Over the Sahelian region, a decrease in the moisture transported by a weak West African westerly jet (WAWJ in **Figure 2**) leads to drought (125).

Upstream planetary wave activity and associated ARs have been implicated in studies of heavy precipitation over South Africa brought on by tropical temperate troughs (TTTs) (126). During summers with good rainfall, the heat low over southern Angola low is prominent and often acts as the tropical source region for the TTTs. During drought conditions, anticyclonic conditions tend to exist over southern Africa, the Angola low is weak, and the TTTs are preferably located over the Southwest Indian Ocean, whereas those TTTs that occur over the mainland tend to be weaker than in wet summers. Many droughts over southern Africa are associated with El Niño events during which the subtropical jet is anomalously far north and the Pacific–South America pattern leads to anticyclonic conditions over southern Africa and the South East Atlantic and reduced likelihood of AR occurrence (**Figure 2**). The role of planetary waves is also highlighted in the evolution of TTTs, as well as the prime moisture source for these systems, which is the tropical Indian Ocean (126). The tropical southeast Atlantic typically acts as a secondary source. Additionally, the importance of latent energy build-up over the Mozambique Channel is also suggested for TTT development (127).

In the southern half of South Africa, most flooding events tend to result from cutoff lows (e.g., 128), but elsewhere in the subcontinent, tropical storms/cyclones are largely the cause (e.g., 129), particularly over Mozambique, Madagascar, Mauritius, and occasionally northeastern South Africa. ARs often are associated with extratropical cyclones and cutoff lows, impinging significant impacts in adjacent continental areas (**Figure 2**). Furthermore, mesoscale convective complexes

(MCCs) (130) have led to flood events in the past, as have intense TTT events (131). Strong LLJs transporting moisture from warm oceanic areas have often been implicated in these events (**Figure 2**). For cutoff lows, LLJs crossing the warm Agulhas Current and reaching the coastal mountains were found to be an important factor in flood events (**Figure 3**) in the Western and Eastern Cape regions of South Africa (128, 132). These events also appeared to show ARs (**Figure 2**) extending south from the Mozambique Channel over the Southwest Indian Ocean and feeding into the flood regions in South Africa (**Figure 3**). A cutoff low interacting with a TTT event in April 2006 led to an LLJ transporting moisture from the equatorial South East Atlantic toward southern Namibia where severe flooding occurred (133).

Moisture inflow from the northern Agulhas Current/southern Mozambique Channel contributed to heavy rainfall associated with MCCs over KwaZulu-Natal/southern Mozambique (134), and from the northern Mozambique Channel for the intense TTT flooding that occurred in Mozambique in January 2013 (130).

In East Africa, an LLJ structure has recently been the focus of some attention (47). The so-called Turkana jet (**Figure 2**) occurs in the Turkana Channel of northern Kenya. The jet occurs semiannually from May to October, being strongest during the June–September dry season, with typical core speeds of approximately 10–15 m/s. The rainfall seems to be modulated by the jet, with strong jets suppressing rainfall during the summer rainy season and favoring droughts in northeast Kenya, southern Somalia, and southeastern Ethiopia.

3.5. Australia and New Zealand

Australian climate is characterized by a vast arid center, encompassed by a wet tropical region in the north and temperate areas in the southwest and southeast. The monsoon is the most significant source of moisture for the northern areas of Australia. It occurs from November to April and is responsible for approximately 90% of the total annual precipitation in the north (135, 136).

The primary source of moisture and rainfall over the southern parts of Australia comes from synoptic systems during wintertime, e.g., cold fronts and embedded cutoff lows. In the southern midlatitudes, Tasmania and New Zealand experience a marked contrast of cloudiness and rainfall from west to east due to their mountainous topography and exposure to westerly winds. Rainfall is highest during austral winter over Tasmania and northern parts of New Zealand but is more evenly distributed throughout the year in the southern parts.

The large-scale transport of moisture in the Australian–New Zealand region is predominantly zonal and occurs to a great extent over the equator and midlatitudes, with zonal migration of those bands throughout all seasons. The western Pacific warm pool, including the Coral Sea (e.g., 6) and north Tasman Sea, is an important source of moisture for eastern Australia. These sources in conjunction with prevailing easterly winds during summer months provide enhanced onshore flow and orographic uplift favoring the occurrence of heavy rain along the eastern seaboard of Australia (137).

The transport of moisture via ARs is not common in Australia, but when ARs occur in the Australian sector, they are not confined to any region in particular (**Figure 2**). In some cases they can be associated with cutoff lows, the Koorin LLJ, Southerly Busters, or LLJs created during the interaction of tropical moisture processes with extratropical weather systems. The strongest and most frequent LLJ in Australia is observed in Daly Water in the Northern Territory and is referred to as the Koorin NLLJ (138). The Koorin jet is associated with easterly winds typically between 15 and 30 m/s in the atmospheric boundary layer and is strongest at night between June and August. It does not show a long, thin flow like those associated with synoptic events or certain terrains; instead, it features a broader horizontal extent than many common LLJs around the world (139). During austral summer, another nocturnal jet forms inland of northwestern Australia. Changes in the direction of this LLJ can modify decisively the moisture available, i.e., to foster more precipitation (northeasterly wind direction with air coming from the Coral Sea) or to favor a drought period (southeasterlies with a continental origin) in west Australia (140). When the latter LLJ wind pattern is associated with a positive phase of the Indian Ocean Dipole, periods of intense droughts have been detected over western, southern, and southeastern Australia (141).

The Southerly Buster (**Figure 2**) is a change in southerly wind that occurs mostly between October and February due to the interaction of a cold front with the Great Dividing Range in southeastern Australia (142, 143). It can produce strong gusts of wind and a dramatic drop in temperature of 10–15°C in less than 1 h. Sydney experienced its strongest Southerly Buster event on December 18, 1948, when a maximum wind gust of 113 km/h was recorded at the city airport. A Southerly Buster event in early February 1977 showed a coastal jet with a width of approximately 150 km over New South Wales, resembling an AR event (142).

AR events can sometimes be accompanied by the development of cutoff lows in the Australian sector (**Figure 2**). Cutoff lows in the Southern Hemisphere occur preferentially over southern Australia and New Zealand between 60°E and 130°W (39, 144), mostly from May to October. A classical formation of a cutoff low was observed in late August 1997, which interacted with a tropical water vapor channel resembling an AR event (145). In that particular case, an LLJ event transported moisture from the Coral Sea to higher latitudes, producing a narrow moist tongue from the tropics to extratropical regions across southeast Australia. The narrow tongue provided an extra supply of moisture to the cutoff low and intensified the weather system, causing heavy rainfall over southern Australia. Many cutoff-low episodes in southern Australia are developed and strengthened by interactions with blocking highs located to their east over the Tasman Sea. In New Zealand, an AR event occurred in early March 1988 during the extratropical transition of tropical cyclone Bola, causing severe damage and floods on the North Island (146). Heavy rainfall exceeding 800 mm in 5 days was recorded on the upwind side of the Gisborne Ranges northeast of New Zealand.

3.6. Indian/South Asian Region

The Asian summer monsoon is a major feature in the general circulation of the globe. The southwest monsoon or the summer monsoon provides approximately 80% of the mean annual rainfall to the various meteorological subdivisions of the Indian continent and is one of the most outstanding meteorological phenomena of them all (147). In a typical monsoon season, the monsoon sets in over the Kerala coast in southwestern India by the first of June and covers the entire Indian subcontinent by the fifteenth of July, withdrawing from northwest India by the first of September. Each monsoon is unique in three important aspects, namely, (*a*) monsoon onset over the Kerala coast, (*b*) active and break periods within the monsoon life cycle (onset-active-weak-break-active-withdrawal), and (*c*) the amount of monsoon rainfall. There have been several studies of the source of moisture for the southwest monsoon rainfall, with the Arabian Sea (e.g., 148) and cross-equatorial flow (e.g., 149) considered the major sources. It is now widely recognized that interhemispheric cross-equatorial flow plays a major role in monsoon activity over the Indian subcontinent.

A study of the role of low-level flow in monsoon activity over the Indian subcontinent using 850-hPa winds showed the importance of low-level flow into the Indian subcontinent (Equatorial Indian Ocean) during active (break) monsoon conditions in two contrasting monsoon years, 1987 (deficit) and 1988 (excess) (150). A strong cross-equatorial LLJ with a core around 850 hPa exists over the Indian Ocean and South Asia during the summer monsoon season (June–September) (62).

Swapna et al.'s (150) study showed that the axis of the LLJ moved away from (toward) the Indian subcontinent during monsoon onset and break (active) periods of the monsoon. A decrease in the strength of this LLJ has been shown to favor drought conditions over the Indian subcontinent (151).

The roles of the Southern Hemispheric Equatorial Trough (SHET) and the Eastern Equatorial Indian Ocean (EEIO) in monsoon activity have been studied using a suite of in situ, satellite, and reanalysis datasets (152). This study revealed that the EEIO is the warmest region in the North Indian Ocean compared with the Arabian Sea and the Bay of Bengal. The sea surface temperature over the EEIO increased by approximately 1°C during the period 1951–2007, which in turn altered the large-scale ocean-atmosphere circulation processes and intensified the SHET and the moisture convergence in the region. This then resulted in a weakened southwest monsoon flow; i.e., a decrease in moisture transport from the Indian Ocean to the Indian subcontinent. By analyzing daily rainfall data, the study also showed an increase in the prolonged break in monsoon conditions during the peak monsoon months of July and August in recent decades. These decadal-scale changes are consistent across several ocean-atmosphere parameters. Although it can be concluded that the increasing trend of break monsoon conditions over the subcontinent is related to ocean-atmosphere processes, further study is needed to fully comprehend the causative mechanisms that have altered the ocean-atmosphere coupling system.

The convective systems over the Northwest Pacific (NWP) region were found to play an important role in all aspects of the monsoon such as the monsoon over Kerala, active-break cycles, and the amount of monsoon rainfall (153). This study revealed that the convective systems were absent for approximately five pentads prior to and after the monsoon over Kerala during excess monsoon years. It also showed that there were twice as many convective systems over the NWP than over the Bay of Bengal region during deficit monsoon years and prolonged breaks in monsoon conditions. Such a scenario occurred in 2009 when there were approximately 18 convective systems over the NWP compared to only three in the North Indian Ocean (of which two formed in the Bay of Bengal). During the summer of 2009, the Indian subcontinent witnessed one of the most severe monsoon droughts in recent years with a seasonal deficit of 23% (making it second only to 1972, which had a deficit of 24%). A southward component in the moisture flux reduces the normal transport of moisture from the Indian Ocean, Arabian Sea, and Bay of Bengal (154).

4. SUMMARY AND FUTURE CHALLENGES

The analysis of the impacts of ARs and LLJs at the regional scale requires an explanation capable of representing the pan-global nature of the phenomena involved. This is attempted in **Figure 3**, which provides a graphical summary of the general impacts of precipitation extremes linked to ARs (blue) and LLJs (red), thereby providing useful information for hydrologists and policymakers.

Some of the most interesting potential future directions of AR studies lie perhaps in the area of multiscale interactions, given the dynamic processes that cause ARs to span a wide range of spatial scales, from planetary-scale circulations to mesoscale frontal waves (41). Furthermore, once an AR makes landfall, much smaller hydrological scales (watershed to hillslope) become relevant. Further work to understand the dynamical processes that lead to the formation of ARs (which would remove the subjectivity inherent in their identification) is also sorely needed. In this regard, the work of Newman et al. (155) moves away from the traditional definition based on shape to one that includes all "episodic poleward-moving moisture plumes," which is more in line with traditional definitions of atmospheric phenomena. In addition, Dacre et al. (156) analyzed selected cases of water vapor transport within a climatology of North Atlantic winter extratropical cyclones, introducing some skepticism to the widely accepted paradigm of the structural definition of ARs.

They discussed the possibility that ARs are formed by a cold front that sweeps up water vapor in the warm sector as it catches up with a warm front. This causes a narrow band of moisture to form with a high water vapor content ahead of the cold front at the base of the WCB airflow. In this framework, water vapor in the warm sector of the cyclone, rather than the long-distance transport of water vapor from the subtropics/tropics, is responsible for the generation of filaments with a high water vapor content. However, the origin of the warm sector associated with most of the water vapor observed in ARs is at odds with recent results obtained using Lagrangian methods (115). The use of Lagrangian analysis is useful for assessing more precisely the sources of moisture associated with ARs. Ramos et al. (115) analyzed 35 years of data allowing them to pinpoint where those ARs arriving in five different domains in Western Europe (Iberian Peninsula, France, the United Kingdom, Southern Scandinavia and the Netherlands, and Northern Scandinavia) uptake moisture abnormally. Their results confirm the important role played by the long-range advection of anomalously uptaken moisture linked to ARs from tropical and subtropical areas between the Caribbean Sea and northern Africa. Future studies of ARs should also allow a more in-depth evaluation of the moisture sources for ARs from a Lagrangian point of view for other regions as well. There are also some important improvements needed for future studies of LLJs, particularly the need to increase the number of observations and the collection of data in specific places to better understand their structure and physical mechanisms. A better exploration of the role of complex terrain on LLJ development and its impact continues to be a challenge. Furthermore, there is a critical need to understand the hydrological impacts in terms of soil moisture, snow accumulation, streamflow, and flooding that occur once AR precipitation reaches watershed.

Most of the extreme precipitation events that occur in Western Europe and the western United States are associated with winter AR events and in South America with LLJs. Both ARs and LLJs have been implicated in flooding events in subtropical southern Africa. Any study that aims to evaluate the changes in flood risk in these domains must take into account the potential role of AR response under different future climate change scenarios. For example, using multiple simulations (45) showed that the North Atlantic ARs affecting the United Kingdom are expected to become stronger and more frequent under different future scenarios. Similarly, Warner et al. (157) showed that precipitation caused by extreme ARs will increase in the western United States under warmer climate scenarios. For LLJs, integrations using regional models have been used to good effect to evaluate the future impacts associated with LLJs; for example, Soares & Marengo (158) suggested for 2071–2100 for the A2 scenario that there could be a greater intensity of moisture transport from tropical regions available to feed the MCCs in the subtropical La Plata River Basin, due to the intense southward flow associated with a faster SALLJ bringing more moisture from the Amazon basin southward. A more intense SALLJ in a warming climate suggests an increased transport of moisture from the north to southeast of the Andes and an increase in the frequency of rainfall extremes in southeastern South America around the exit region of the LLJ.

Finally, special consideration should be given in future studies to the role of ARs in the highly sensitive (to climate change) regions of the Arctic and the Antarctic. For example, heavy snow accumulation in East Antarctica during 2009 and 2011 contributed significantly to the mass balance of the Antarctic ice sheet surface. Precipitation during these two years was associated with a few ARs that contributed to nearly 80% of the outstanding ice sheet surface mass balance (159).

DISCLOSURE STATEMENT

The authors are not aware of any affiliations, memberships, funding, or financial holdings that might be perceived as affecting the objectivity of this review.

ACKNOWLEDGMENTS

Francina Dominguez was supported by NASA Award number NNX14AD77G. Raquel Nieto acknowledges the support of the Spanish government and the Xunta de Galicia through their funding of the TRAMO (CGL-2012-35485) and THIS (EM2014/043) projects, respectively, which are also funded by FEDER (European Regional Development Fund), and the CNPq grant 314734/2014-7 by the Brazilian government. Anita Drumond acknowledges funding by the Spanish government and FEDER through the SETH (CGL2014-60849-JIN) project. Alexandre M. Ramos was supported through a postdoctoral grant (SFRH/BPD/84328/2012) through FCT (Fundação para a Ciência e a Tecnologia, Portugal). José Marengo was funded by the National Institute of Science and Technology for Climate Change INCT-MC by CNPq grant 573797/2008-0, FAPESP grant 2008/57719-9, FAPESP RCUK PULSE grant 2011/51843-2, and the CNPq-PRIMO project. Andréa Taschetto is supported by the Australian Research Council.

LITERATURE CITED

1. Peixoto JP, Oort AH. 1992. *Physics of Climate*. New York: Am. Inst. Phys. 520 pp.
2. Yu L, Weller RA. 2007. Objectively analyzed air-sea heat fluxes for the global ice-free oceans (1981–2005). *Bull. Am. Meteor. Soc.* 88:527–39
3. Trenberth KE, Dai A, Rasmussen RM, Parsons DB. 2003. The changing character of precipitation. *Bull. Am. Meteor. Soc.* 84:1205–17
4. Bales RC. 2003. Hydrology: overview. In *Encyclopedia of Atmospheric Sciences*, ed. GR North, JA Pyle, F Zhang, pp. 968–73. Philadelphia: Elsevier. 2nd ed.
5. Stocker TF, Qin D, Plattner G-K, Tignor MMB, Allen SK, et al. 2013. *Climate Change 2013: The Physical Science Basis. Working Group I Contribution to the Fifth Assessment Report of the Intergovernmental Panel on Climate Change. Summary for Policymaker*s. Geneva, Switz.: Intergov. Panel Climate Change
6. Gimeno L, Drumond A, Nieto R, Trigo RM, Stohl A. 2010. On the origin of continental precipitation. *Geophys. Res. Lett.* 37:L13804
7. Gimeno L, Stohl A, Trigo RM, Dominguez F, Yoshimura K, et al. 2012. Oceanic and terrestrial sources of continental precipitation. *Rev. Geophys.* 50(4):RG4003
8. Gimeno L, Nieto R, Drumond A, Castillo R, Trigo RM. 2013. Influence of the intensification of the major oceanic moisture sources on continental precipitation. *Geophys. Res. Lett.* 40:1–8
9. Dominguez F, Praveen K, Vivoni ER. 2008. Precipitation recycling variability and ecoclimatological stability—a study using NARR data. Part II: North American monsoon region. *J. Clim.* 21:5187–203
10. Trigo RM, Añel J, Barriopedro D, García-Herrera R, Gimeno L, et al. 2013. The record winter drought of 2011–12 in the Iberian Peninsula, in explaining extreme events of 2012 from a climate perspective. *Bull. Am. Meteor. Soc.* 94(9):S41–S45
11. Stohl A, James P. 2004. A Lagrangian analysis of the atmospheric branch of the global water cycle. Part I: method description, validation, and demonstration for the August 2002 flooding in Central Europe. *J. Hydrometeor*. 5:656–78
12. Stensrud DJ. 1996. Importance of low-level jets to climate. *J. Clim.* 9:1698–711
13. Marengo JA, Soares WR, Saulo S, Nicolini M. 2004. Climatology of the low-level jet east of the Andes as derived from the NCEP–NCAR reanalyses: characteristics and temporal variability. *J. Clim.* 17:2261–80
14. Gimeno L, Nieto R, Vazquez M, Lavers D. 2014. Atmospheric rivers: a minireview. *Front. Earth Sci.* 2:2
15. Dettinger MD, Ralph FM, Das T, Neiman PJ, Cayan DR. 2011. Atmospheric rivers, floods and the water resources of California. *Water* 3:445–78
16. Lavers DA, Allan RP, Wood EF, Villarini G, Brayshaw DJ, Wade AJ. 2011. Winter floods in Britain are connected to atmospheric rivers. *Geophys. Res. Lett.* 38:L23803
17. Trigo RM, Varino F, Ramos AM, Valente MA, Zêzere JL, et al. 2014. The record precipitation and flood event in Iberia in December 1876: description and synoptic analysis. *Front. Earth Sci.* 2:3
18. Vera C, Higgins W, Amador J, Ambrizzi T, Garreaud R, et al. 2006. Toward a unified view of the American monsoon systems. *J. Clim.* 19:4977–5000

19. Thorncroft CD, Nguyen H, Zhang C, Peyrillé P. 2011. Annual cycle of the West African monsoon: regional circulations and associated water vapour transport. *Q. J. Roy. Meteor. Soc.* 137:129–47
20. Redmond KT. 2002. The depiction of drought. *Bull. Am. Meteor. Soc.* 83:1143–47
21. Stohl A, Forster C, Sodemann H. 2008. Remote sources of water vapor forming precipitation on the Norwegian west coast at 60°N: a tale of hurricanes and an atmospheric river. *J. Geophys. Res.* 113:D05102
22. Seneviratne SI, Lüthi D, Litschi M, Schär C. 2006. Land-atmosphere coupling and climate change in Europe. *Nature* 443:205–9
23. Coelho CS, Oliveira C, Ambrizzi T, Reboita M, Carpenedo C, et al. 2015. The 2014 southeast Brazil austral summer drought: regional scale mechanisms and teleconnections. *Clim. Dyn.* 45:1–16
24. Zhu Y, Newell RE. 1998. A proposed algorithm for moisture fluxes from atmospheric rivers. *Mon. Weather Rev.* 126:725–35
25. Newell RE, Newell NE, Zhu Y, Scott C. 1992. Tropospheric rivers?—a pilot study. *Geophys. Res. Lett.* 19(24):2401–4
26. Knippertz P, Wernli H. 2010. A Lagrangian climatology of tropical moisture exports to the Northern hemispheric extratropics. *J. Clim.* 23:987–1003
27. Bao J-W, Michelson SA, Neiman PJ, Ralph FM, Wilczak JM. 2006. Interpretation of enhanced integrated water vapor bands associated with extratropical cyclones: their formation and connection to tropical moisture. *Mon. Weather Rev.* 134:1–18
28. Lackmann GM, Gyakum JR. 1999. Heavy cold-season precipitation in the northwestern United States: synoptic climatology and an analysis of the flood of 17–18 January 1986. *Weather Forecast*. 14(5):687–700
29. Dirmeyer PA, Kinter JLIII, Michalak AM, Jackson R. 2009. The "Maya Express": floods in the US Midwest. *EOS* 90(12):101–2
30. Arraut JM, Nobre C, Barbosa H, Obregon G, Marengo J. 2012. Aerial rivers and lakes: looking at large-scale moisture transport and its relation to Amazonia and to subtropical rainfall in South America. *J. Clim.* 25:543–56
31. Rivera ER, Dominguez F, Castro CL. 2014. Atmospheric rivers and cool season extreme precipitation events in the Verde River basin of Arizona. *J. Hydrometeorol.* 15:813–29
32. Cavazos T, Rivas D. 2004. Variability of extreme precipitation events in Tijuana, Mexico. *Clim. Res.* 25:229–43
33. Carlson TN. 1980. *Mid-Latitude Weather Systems*. London: HarperCollins Acad.
34. Ralph FM, Neiman PJ, Rotunno R. 2005. Dropsonde observations in low-level jets over the Northeastern Pacific Ocean from CALJET-1998 and PACJET-2001: mean vertical-profile and atmospheric-river characteristics. *Mon. Weather Rev.* 133:889–910
35. Ralph FM, Neiman PJ, Wick GA. 2004. Satellite and CALJET aircraft observations of atmospheric rivers over the eastern North Pacific Ocean during the winter of 1997/98. *Mon. Weather Rev.* 132:1721–45
36. Dettinger M, Ralph FM, Lavers D. 2015. Setting the stage for a global science of atmospheric rivers. *EOS* 96. doi:10.1029/2015EO038675
37. Wick GA, Neiman PJ, Ralph FM. 2013. Description and validation of an automated objective technique for identification and characterization of the integrated water vapor signature of atmospheric rivers. *IEEE Trans. Geosci. Remote Sensing* 51(4):2166–76
38. Ramos AM, Trigo RM, Liberato MLR, Tomé R. 2015. Daily precipitation extreme events in the Iberian Peninsula and its association with atmospheric rivers. *J. Hydrometeor.* 16:579–97
39. Guan B, Waliser DE. 2015. Detection of atmospheric rivers: evaluation and application of an algorithm for global studies. *J. Geophys. Res. Atmos.* 120(24):12514–35
40. Lavers DA, Villarini G, Allan RP, Wood EF, Wade AJ. 2012. The detection of atmospheric rivers in atmospheric reanalyses and their links to British winter floods and the large-scale climatic circulation. *J. Geophys. Res.* 117:D20106
41. Ralph FM, Neiman PJ, Kiladis GN, Weickmann K, Reynolds DW. 2011. A multiscale observational case study of a pacific atmospheric river exhibiting tropical-extratropical connections and a mesoscale frontal wave. *Mon. Weather Rev.* 139:1169–89
42. Ralph FM, Dettinger MD. 2011. Storms, floods, and the science of atmospheric rivers. *EOS* 92(32):265–66

43. Dettinger MD. 2004. *Fifty-two years of "pineapple-express" storms across the West Coast of North America*. PIER Project Rep. CEC-500-2005-004 2, US Geol. Surv., Scripps Inst. Oceanogr. Calif. Energy Comm.
44. Lavers DA, Villarini G. 2013. The nexus between atmospheric rivers and extreme precipitation across Europe. *Geophys. Res. Lett.* 40:3259–64
45. Lavers DA, Allan RP, Villarini G, Lloyd-Hughes B, Brayshaw DJ, Wade AJ. 2013. Future changes in atmospheric rivers and their implications for winter flooding in Britain. *Environ. Res. Lett.* 8:034010
46. Liepert BG. 2013. Atmospheric rivers in changing climate. *Environ. Res. Lett.* 8(3):031006
47. Nicholson S. 2016. The Turkana low-level jet: mean climatology and association with regional aridity. *Int. J. Climatol.* 36:2598–614
48. Blackadar AK. 1957. Boundary layer wind maxima and their significance for the growth of nocturnal inversions. *Bull. Am. Meteor. Soc.* 38:283–90
49. Bonner WD. 1968. Climatology of the low-level jet. *Mon. Weather Rev.* 96:833–50
50. Whiteman CD, Bian X, Zhong S. 1997. Low-level jet climatology from enhanced rawinsonde observations at a site in the Southern Great Plains. *J. Appl. Meteor.* 36:1363–76
51. Jiang Q, Wang S, O'Neil L. 2010. Some insights into the characteristics and dynamics of the Chilean low-level coastal jet. *Mon. Weather Rev.* 138:3185–206
52. Parish T. 2000. Forcing of the summer low-level jet along the California coast. *J. Appl. Meteorol.* 39:2421–33
53. Liu M, Westphal DL, Holt TR, Xu Q. 2000. Numerical simulation of a low-level jet over complex terrain in southern Iran. *Mon. Weather Rev.* 128:1309–27
54. Rife DL, Pinto JO, Monaghan AJ, Davis CA, Hannon JR. 2010. Global distribution and characteristics of diurnally varying low-level jets. *J. Clim.* 23:5041–64
55. Mo KC, Berbery EH. 2004. Low-level jets and the summer precipitation regimes over North America. *J. Geophys. Res.* 109:D06117
56. Higgins RW, Yao Y, Yarosh ES, Janowiak JE, Mo KC. 1997. Influence of the Great Plains low-level jet on summertime precipitation and moisture transport over the central United States. *J. Clim.* 10:481–507
57. Vera C, Baez J, Douglas M, Emmanuel CB, Marengo J, et al. 2006. The South American low-level jet experiment. *Bull. Am. Meteor. Soc.* 87:63–77
58. Rotunno R. 1983. On the linear theory of land and sea breeze. *J. Atmos. Sci.* 40:1999–2009
59. Wallace J. 1975. Diurnal variations in precipitation and thunderstorm frequency over the conterminous United States. *Mon. Weather Rev.* 103:406–19
60. Nogues-Paegle J, Mo KC. 1997. Alternating wet and dry conditions over South America during summer. *Mon. Weather Rev.* 125:279–91
61. Zhang C, Woodworth P, Guojun G. 2006. The seasonal cycle in the lower troposphere over West Africa from sounding observations. *Q. J. Roy. Meteor. Soc.* 132:2559–82
62. Joseph PV, Sijikumar S. 2004. Intraseasonal variability of the low level jet stream of Asian summer monsoon. *J. Clim.* 17:1449–58
63. Miller D, Fritsch JM. 1991. Mesoscale convective complexes in the western Pacific region. *Mon. Weather Rev.* 119:2978–92
64. Monaghan AJ, Rife DL, Pinto JO, Davis CA, Hannan JR. 2010. Global precipitation extremes associated with diurnally varying low-level jets. *J. Clim.* 23:5065–84
65. Benton GS, Estoque MA. 1954. Water-vapor transfer over the North American continent. *J. Meteorol.* 11:462–77
66. Helfand HM, Schubert SD. 1995. Climatology of the simulated Great Plains low-level jet and its contribution to the continental moisture budget of the United States. *J. Clim.* 8:784–806
67. Anderson BT, Roads JO, Chen S-C, Juang H-M. 2000. Regional simulation of the low-level monsoon winds over the Gulf of California and southwestern United States. *J. Geophys. Res.* 105:17955–69
68. Brenner IS. 1974. A surge of maritime tropical air—Gulf of California to the Southwestern United States. *Mon. Weather Rev.* 102:375–89
69. Fuller RD, Stensrud DJ. 2000. The relationship between tropical easterly waves and surges over the Gulf of California during the North American monsoon. *Mon. Weather Rev.* 128:2983–89
70. Higgins RW, Shi W, Hain C. 2004. Relationships between Gulf of California moisture surges and precipitation in the Southwestern United States. *J. Clim.* 17:2983–97

71. Carleton AM. 1986. Synoptic-dynamic character of "bursts" and "breaks" in the southwest U.S. summer precipitation singularity. *J. Clim.* 6:605–23
72. Cavazos T, Comrie AC, Liverman DM. 2002. Intraseasonal anomalies associated with wet monsoons in southeast Arizona. *J. Clim.* 15:2477–90
73. Anderson BT, Roads JO, Chen S-C. 2000. Large-scale forcing of summertime monsoon surges over the Gulf of California and the southwestern United States. *J. Geophys. Res.* 105:24455–67
74. Douglas MW, Leal JC. 2003. Summertime surges over the Gulf of California: aspects of their climatology, mean structure, and evolution from radiosonde, NCEP reanalysis, and rainfall data. *Weather Forecast* 18:55–74
75. Higgins RW, Shi W. 2005. Relationships between Gulf of California moisture surges and tropical cyclones in the Eastern Pacific basin. *J. Clim.* 18:4601–20
76. Hu H, Dominguez F. 2015. Evaluation of oceanic and terrestrial sources of moisture for the North American monsoon using numerical models and precipitation stable isotopes. *J. Hydrometeorol.* 16:19–35
77. Mo KC, Nogues-Paegle J, Paegle J. 1995. Physical mechanisms of the 1993 summer floods. *J. Atmos. Sci.* 52:879–95
78. Arritt RW, Rink TD, Segal M, Todey DP, Clark CA. 1997. The Great Plains low-level jet during the warm season of 1993. *Mon. Weather Rev.* 125:1–17
79. Dirmeyer PA, Kinter JL. 2010. Floods over the US Midwest: a regional water cycle perspective. *J. Hydrometeorol.* 11:1172–81
80. Dirmeyer PA, Brubaker KL, DelSole T. 2009. Import and export of atmospheric water vapor between nations. *J. Hydrol.* 365:11–22
81. Mestas-Nuñez AM, Enfield DB, Zhang C. 2007. Water vapor fluxes over the Intra-Americas Sea: seasonal and interannual variability and associations with rainfall. *J. Clim.* 20:1910–22
82. Lavers DA, Villarini G. 2013. Atmospheric rivers and flooding over the Central United States. *J. Clim.* 26:7829–36
83. Barandiaran D, Wang SY, Hilburn K. 2013. Observed trends in the Great Plains low-level jet and associated precipitation changes in relation to recent droughts. *Geophys. Res. Lett.* 40:6247–51
84. Ralph FM, Neiman PJ, Wick GA, Gutman SI, Dettinger MD, et al. 2006. Flooding on California's Russian River: role of atmospheric rivers. *Geophys. Res. Lett.* 33:L13801
85. Neiman PJ, Ralph FM, Wick GA, Lundquist JD, Dettinger MD. 2008. Meteorological characteristics and overland precipitation impacts of atmospheric rivers affecting the West Coast of North America based on eight years of SSM/I satellite observations. *J. Hydrometeorol.* 9:22–47
86. Neiman PJ, Schick LJ, Ralph FM, Hughes M, Wick GA. 2011. Flooding in western Washington: the connection to atmospheric rivers. *J. Hydrometeorol.* 12:1–22
87. Hughes M, Mahoney KM, Neiman PJ, Moore BJ, Alexander M, Ralph FM. 2014. The landfall and inland penetration of a flood-producing atmospheric river in Arizona. Part II: sensitivity of modeled precipitation to terrain height and atmospheric river orientation. *J. Hydrometeorol.* 15:1954–74
88. Neiman PJ, Ralph FM, Moore BJ, Hughes M, Mahoney KM, et al. 2013. The landfall and inland penetration of a flood-producing atmospheric river in Arizona. Part I: observed synoptic-scale, orographic, and hydrometeorological characteristics. *J. Hydrometeorol.* 14:460–84
89. Rutz JJ, Steenburgh WJ. 2012. Quantifying the role of atmospheric rivers in the interior western United States *Atmos. Sci. Lett.* 13:257–61
90. Knippertz P, Martin JE. 2007. A Pacific moisture conveyor belt and its relationship to a significant precipitation event in the semiarid Southwestern United States. *Weather Forecast* 22:125–44
91. Dettinger MD. 2013. Atmospheric rivers as drought busters on the U.S. West Coast. *J. Hydrometeor.* 14:1721–32
92. Dettinger MD, Ingram BL. 2013. The coming mega storms. *Sci. Amer.* 308:64–71
93. Amador JA. 2008. The Intra-Americas Sea low-level jet. *Ann. N. Y. Acad. Sci.* 1146:153–88
94. Poveda G, Mesa OJ. 1999. The CHOCO low-level jet and two others jets over Colombia: climatology and variability during ENSO [in Spanish]. *Rev. Acad. Colomb. Cienc.* 23(89):517–28
95. Poveda G, Jaramillo L, Vallejo LF. 2014. Seasonal precipitation patterns along pathways of South American low-level jets and aerial rivers. *Water Resour. Res.* 50:98–118

96. Sakamoto MS, Ambrizzi T, Poveda G. 2011. Moisture sources and life cycle of convective systems over western Colombia. *Adv. Meteorol.* 2011:1–11
97. Durán-Quesada AM, Gimeno L, Amador JA, Nieto R. 2010. Moisture sources for Central America: identification of moisture sources using a Lagrangian analysis technique. *J. Geophys. Res.* 115:D05103
98. Marengo JA. 2005. Characteristics and spatio-temporal variability of the Amazon River Basin Water Budget. *Clim. Dyn.* 24:11–22
99. Drumond A, Nieto R, Gimeno L, Ambrizzi T. 2008. A Lagrangian identification of major sources of moisture over Central Brazil and La Plata Basin. *J. Geophys. Res.* 113:D14128
100. Drumond A, Marengo J, Ambrizzi T, Nieto R, Moreira L, Gimeno L. 2014. The role of the Amazon Basin moisture in the atmospheric branch of the hydrological cycle: a Lagrangian analysis. *Hydrol. Earth Syst. Sci.* 18:2577–98
101. Arraut JM, Satyamurty P. 2009. Precipitation and water vapor transport in the Southern Hemisphere with emphasis on the South American region. *J. Appl. Meteor. Climatol.* 48:1902–12
102. Martinez JA, Dominguez F. 2014. Sources of atmospheric moisture for the La Plata River Basin. *J. Clim.* 27:6737–53
103. Marengo JA, Nobre CA, Tomasella J, Oyama MD, Oliveira GS, et al. 2008. The drought of Amazonia in 2005. *J. Clim.* 21:495–516
104. Marengo JA. 2006. On the hydrological cycle of the Amazon Basin: a historical review and current state-of-the-art. *Rev. Brasil. Meteorol.* 21:1–19
105. Zemp DC, Schleussner C-F, Barbosa HMJ, van der Ent RJ, Donges JF, et al. 2014. On the importance of cascading moisture recycling in South America. *Atmos. Chem. Phys.* 14:13337–59
106. Spracklen DV, Arnold SR, Taylor CM. 2012. Observations of increased tropical rainfall preceded by air passage over forests. *Nature* 489:282–85
107. Marengo JA, Espinoza JC. 2016. Extreme seasonal droughts and floods in Amazonia: causes, trends and impacts. *Int. J. Climatol.* 36:1033–50
108. Viale M, Nuñez MN. 2011. Climatology of winter orographic precipitation over the subtropical Central Andes and associated synoptic and regional characteristics. *J. Hydrometeor.* 12:481–507
109. Falvey M, Garreaud R. 2007. Wintertime precipitation episodes in Central Chile: associated meteorological conditions and orographic influences. *J. Hydrometeor.* 8:171–93
110. Liberato MLR, Ramos AM, Trigo RM, Trigo IF, Durán-Quesada AM, et al. 2013. Moisture sources and large-scale dynamics associated with a flash flood event. In *Lagrangian Modeling of the Atmosphere*, ed. J Lin, D Brunner, C Gerbig, A Stohl, A Luhar, P Webley, pp. 111–26. Washington, DC: Am. Geophys. Union
111. Lavers DA, Villarini G. 2015. The contribution of atmospheric rivers to precipitation in Europe and the United States. *J. Hydrol.* 522:382–90
112. Eiras-Barca J, Brands S, Miguez-Macho G. 2016. Seasonal variations in North Atlantic atmospheric river activity and associations with anomalous precipitation over the Iberian Atlantic Margin. *J. Geophys. Res. Atmos.* 121:931–48
113. Couto FT, Salgado R, Costa MJ, Prior V. 2015. Precipitation in the Madeira Island over a 10-year period and the meridional water vapour transport during the winter seasons. *Int. J. Climatol.* 35:3748–59
114. Sodemann H, Stohl A. 2013. Moisture origin and meridional transport in atmospheric rivers and their association with multiple cyclones. *Mon. Weather Rev.* 141:2850–68
115. Ramos AM, Nieto R, Tomé R, Gimeno L, Trigo RM, et al. 2016. Atmospheric rivers moisture sources from a Lagrangian perspective. *Earth Syst. Dyn.* 7:371–84
116. Zêzere JL, Pereira S, Tavares AO, Bateira C, Trigo RM, et al. 2014. DISASTER: a GIS database on hydro-geomorphologic disasters in Portugal. *Nat. Hazards* 72:503–32
117. Pereira S, Ramos AM, Zêzere JL, Trigo RM, Vaquero JM. 2015. Spatial impact and triggering conditions of the exceptional hydro-geomorphological event of December 1909 in Iberia. *Nat. Hazards Earth Syst. Sci. Discuss.* 3:5805–45
118. Couto FT, Salgado R, Costa MJ. 2012. Analysis of intense rainfall events on Madeira Island during the 2009/2010 winter. *Nat. Hazards Earth Syst. Sci.* 12:2225–40
119. Ranjha R, Svensson G, Tjernström M, Semedo A. 2013. Global distribution and seasonal variability of coastal low-level jets derived from ERA-Interim reanalysis. *Tellus A* 65:20412

120. Christakos K, Varlas G, Reuder J, Katsafados P, Papadopoulos A. 2014. Analysis of a low-level coastal jet off the Norwegian coast. *Energy Procedia* 53:162–72
121. Mason SJ, Jury MR. 1997. Climatic variability and change over southern Africa: a reflection on underlying processes. *Prog. Phys. Geogr.* 21:23–50
122. Blamey R, Reason CJC. 2007. Relationships between Antarctic sea-ice and South African winter rainfall. *Clim. Res.* 33:183–93
123. D'Abreton P, Tyson P. 1995. Divergent and non-divergent water vapour transport over southern Africa during wet and dry conditions. *Meteor. Atmos. Phys.* 55:47–59
124. Cook C, Reason CJC, Hewitson BC. 2004. Wet and dry spells within particular wet and dry summers in the South African summer rainfall region. *Clim. Res.* 26:17–31
125. Pu B, Cook KH. 2012. Role of the West African westerly jet in Sahel rainfall variations. *J. Clim.* 25:2880–96
126. Hart NCG, Reason CJC, Fauchereau N. 2010. Tropical-extratropical interactions over southern Africa: three cases of heavy summer season rainfall. *Mon. Weather Rev.* 138:2608–23
127. Macron C, Pohl B, Richard Y, Bessafi M. 2014. How do tropical temperate troughs form and develop over southern Africa? *J. Clim.* 27:1633–47
128. Singleton AT, Reason CJC. 2007. Variability in the characteristics of cut-off low pressure systems over subtropical southern Africa. *Int. J. Climatol.* 27:295–310
129. Klinman M, Reason CJC. 2008. On the peculiar storm track of TC Favio during the 2006–2007 Southwest Indian Ocean tropical cyclone season and relationships to ENSO. *Met. Atmos. Phys.* 100:233–42
130. Blamey RC, Reason CJC. 2013. The role of mesoscale convective complexes in southern Africa summer rainfall. *J. Clim.* 26:1654–68
131. Manhique A, Reason CJC, Silinto B, Zucula J, Raiva I, et al. 2015. Extreme rainfall and floods in southern Africa in January 2013 and associated circulation patterns. *Nat. Hazards* 77(2):679–91
132. Singleton AT, Reason CJC. 2006. Numerical simulations of a severe rainfall event over the Eastern Cape coast of South Africa: sensitivity to sea surface temperature and topography. *Tellus A* 58(3):355–67
133. Muller A, Reason CJC, Fauchereau N. 2008. Extreme rainfall in the Namib desert during late summer 2006 and influences of regional ocean variability. *Int. J. Climatol.* 28:1061–70
134. Blamey R, Reason CJC. 2009. Numerical simulation of a mesoscale convective system over the east coast of South Africa. *Tellus A* 61:17–34
135. Smith IN, Wilson L, Suppiah R. 2008. Characteristics of the Northern Australian rainy season. *J. Clim.* 21(17):4298–311
136. Pope M, Jakob C, Reeder MJ. 2009. Regimes of the north Australian wet season. *J. Clim.* 22(24):6699–715
137. Black MT, Lane TP. 2015. An improved diagnostic for summertime rainfall along the eastern seaboard of Australia. *Int. J. Climatol.* 35:80–92
138. Allen SC. 1980. Observational characteristics of the low-level jet at Daly Waters during Project Koorin. *Aust. Meteorol. Mag.* 28:47–56
139. Brook RR. 1985. The Koorin nocturnal low-level jet. *Boundary-Layer Meteorol.* 32(2):133–54
140. Ackerley D, Berry G, Jakobb C, Reedera MJ. 2014. The roles of diurnal forcing and large-scale moisture transport for initiating rain over northwest Australia in a GCM. *Q. J. R. Meteorol. Soc.* 140:2515–26
141. Ummenhofer CC, England MH, McIntosh PC, Meyers GA, Pook MJ, et al. 2009. What causes southeast Australia's worst droughts? *GRL* 36:L04706
142. Baines PG. 1980. The dynamics of the Southerly Buster. *Aust. Meteor. Mag.* 28(4):175–200
143. McInnes KL, McBride JL. 1993. Australian Southerly Busters. Part I. Analysis of a numerically simulated case study. *Mon. Weather Rev.* 121(7):1904–20
144. Reboita MS, Nieto R, Gimeno L, Da Rocha RP, Ambrizzi T, et al. 2010. Climatological features of cutoff low systems in the Southern Hemisphere. *J. Geophys. Res. Atmos.* 115:D17104
145. Qi L, Leslie LM, Zhao SX. 1999. Cut-off low pressure systems over southern Australia: climatology and case study. *J. Clim.* 19(15):1633–49
146. Sinclair MR. 1993. A diagnostic study of the extratropical precipitation resulting from Tropical Cyclone Bola. *Mon. Weather Rev.* 121(10):2690–707

147. Ananthakrishnan R, Pathan JM. 1981. *Pentad rainfall charts and space time variations of rainfall over India and the adjoining areas*. Res. Rep. 036, Ramdurg House, Ind. Inst. Trop. Meteor., Pune, Ind. **http://www.tropmet.res.in/~lip/Publication/RR-pdf/RR-36.pdf**
148. Pisharoty PR. 1965. Evaporation from the Arabian Sea and Indian southwest monsoon. In *Proceedings of the Symposium on Meteorological Results of IIOE*, ed. Pisharotypp PR, pp. 43–54. Bombay, India: Int. Indian Ocean Exped. Meteorol. Dep.
149. Ramesh Kumar MR, Schluessel P. 1998. Air sea interaction over the Indian Ocean during the two contrasting monsoon years 1987 and 1988 studied with satellite data. *Theor. Appl. Climatol.* 60:219–31
150. Swapna P, Ramesh Kumar MR. 2002. Role of low level flow on the summer monsoon rainfall over the Indian subcontinent during two contrasting monsoon years. *J. Indian Geophys. Union* 6(3):123–37
151. Joseph PV, Simon A. 2005. Weakening trend of the southwest monsoon current through peninsular India from 1950 to the present. *Curr. Sci.* 89:687–94
152. Ramesh Kumar MR, Krishnan R, Sankar S, Unnikrishnan AS, Pai DS. 2009. Increasing trend of "break-monsoon" conditions over India—role of ocean-atmosphere processes in the Indian Ocean. *IEEE Geosci. Remote Sens. Lett.* 6(2):332–36
153. Ramesh Kumar MR, Babu AK, Reason C. 2009. On the role of convective systems over the northwest Pacific and monsoon activity over the Indian subcontinent. *Meteorol. Appl.* 16:353–60
154. Preethi B, Revadekar JV, Kripalani RH. 2009. Anomalous behaviour of the Indian summer monsoon 2009. *J. Earth Syst. Sci.* 120(5):783–94
155. Newman M, Kiladis GN, Weickmann KM, Ralph FM, Sardeshmukh PD. 2012. Relative contributions of synoptic and low-frequency eddies to time-mean atmospheric moisture transport, including the role of atmospheric rivers. *J. Clim.* 25:7341–61
156. Dacre H, Clark P, Martinez-Alvarado O, Stringer M, Lavers D. 2015. How do atmospheric rivers form? *Bull. Am. Meteor. Soc.* 1243–55
157. Warner MD, Mass CF, Salathé EP Jr. 2015. Changes in winter atmospheric rivers along the North American West Coast in CMIP5 climate models. *J. Hydrometeor.* 16:118–28
158. Soares WR, Marengo JA. 2009. Assessments of moisture fluxes east of the Andes in South America in a global warming scenario. *Int. J. Climatol.* 28:1395–414
159. Gorodetskaya IV, Tsukernik M, Claes K, Ralph MF, Neff WD, Van Lipzig NP. 2014. The role of atmospheric rivers in anomalous snow accumulation in East Antarctica. *Geophys. Res. Lett.* 41(17):6199–206
160. Martins HS, Sá LDA, Moraes OLL. 2013. Low level jets in the Pantanal wetland nocturnal boundary layer—case studies. *Am. J. Environ. Eng.* 3(1):32–47